HYPOTHETICAL ASTEROID 2023 PDC MASS MEASUREMENT VIA DOPPLER GRAVIMETRY IN A RECONNAISSANCE FLYBY Ry Bull[1], J.A. Atchison[1], J.D. Bradfield[1], J. Woodburn[2], [1]Johns Hopkins Applied Physics Laboratory, 11100 Johns Hopkins Road, Laurel, MD 20723 USA; Ry.Bull@jhuapl.edu; [2]AGI, 220 Valley Creek Boulevard, Exton, PA 19341 USA

Keywords: *asteroid flyby missions, gravity science*

Introduction: Rapid reconnaissance flyby missions are a key tool to quickly visiting and characterizing a potentially hazardous asteroid (PHA). Compared to a rendezvous mission, flybys can have more frequent launch opportunities and can arrive at the asteroid faster, which can be critical when a timely response to a threatening object is needed. Due to these factors, the 2022 Planetary Science Decadal survey recommended that the next planetary defense (PD) mission be a demonstration of a rapid reconnaissance flyby [1]. However, due to the nature of a flyby, some important measurements of a PHA are limited or impossible. Three of the most important and most difficult properties to measure are interrelated: mass, density, and porosity. These characteristics are needed in order to estimate the possible damage to Earth as well as to design mitigation strategies [2].

In a typical flyby, asteroid mass is obtained by using Earth-based ranging and Doppler measurements to track the spacecraft as its orbit is perturbed by the asteroid's gravity. However, this technique is limited to asteroids larger than approximately 3-5 km in diameter, even with very favorable flyby conditions. This means that flybys cannot supply precise mass measurements for many of the most concerning asteroids. This includes the hypothetical asteroid for the 2023 PDC impact scenario, 2023 PDC. At the time of discovery, 2023 PDC has an estimated diameter between 220 and 660 meters, making it too small for the asteroid's mass to be observable using Earth-based tracking of the flyby spacecraft.

This study evaluates the feasibility of using a new technique called Doppler Gravimetry (DopGrav) to return a mass measurement from a high-speed spacecraft flyby of 2023 PDC. DopGrav augments the Earth-based tracking with additional Doppler and optical measurements from the spacecraft to one or more test-masses that pass much closer to the asteroid, significantly improving the sensitivity of the mass measurement. Here, we study a test-mass that is a 6U CubeSat, with a concept-of-operations similar to what was recently used by LICIACube and DART [3]. It is deployed by the host spacecraft approximately two weeks prior to the close approach with the asteroid. It has an on-board propulsion system allowing it to perform its own targeting maneuvers to achieve the desired close approach distances with the asteroid. Figure 1 illustrates this concept.

We will show the expected mass measurement performance of this CubeSat-based DopGrav architecture for the proposed reconnaissance flyby mission to 2023 PDC. In this case, we consider only a single CubeSat. In the event that 2023 PDC turns out to be significantly smaller than expected, DopGrav may still provide a meaningful upper bound on the mass, bounding the potential damage and mitigation options.

Motivation: Mass, density, and porosity are used to predict both the impact consequences of a PHA and the effectiveness of different mitigation options. Miller et al. [4] prioritized the list of necessary PHA characteristics needed to react to a threat. The first four (of seven) are: orbit, mass, composition, and porosity. Here, *porosity* refers to the total volumetric fraction of voids within the asteroid of a known or assumed composition. We emphasize the importance of mass and porosity, which are challenging or impossible measure from a flyby.

Asteroid mass gives the total kinetic energy of the impact. Density and porosity help us predict how much of that energy will be lost to the atmosphere on entry [5, 6]. Together, these parameters (with their uncertainties) are needed so damage assessment models can predict the impact effects (blast overpressure, thermal, tsunami, etc.) and determine the size of the region to evacuate [7].

Additionally, When designing a mitigation, the asteroid's mass determines the required momentum for deflection. For a kinetic impactor, asteroid porosity is critical because it affects the shock response [8] and momentum enhancement factor β [9]. Holsapple and Housen [10] found that porosity is "the single greatest influence in the parameters that determine β." Porosity is also an important parameter in predicting the disruption of an object. Porous objects can withstand higher impulses without fragmentation [11, 12]. Likewise, for a deflection using a nuclear explosive device, Gennery *et. al.* [13] found that both the yield and standoff distance should be tailored for the target's porosity. Ultimately, Syal, et al. concludes:

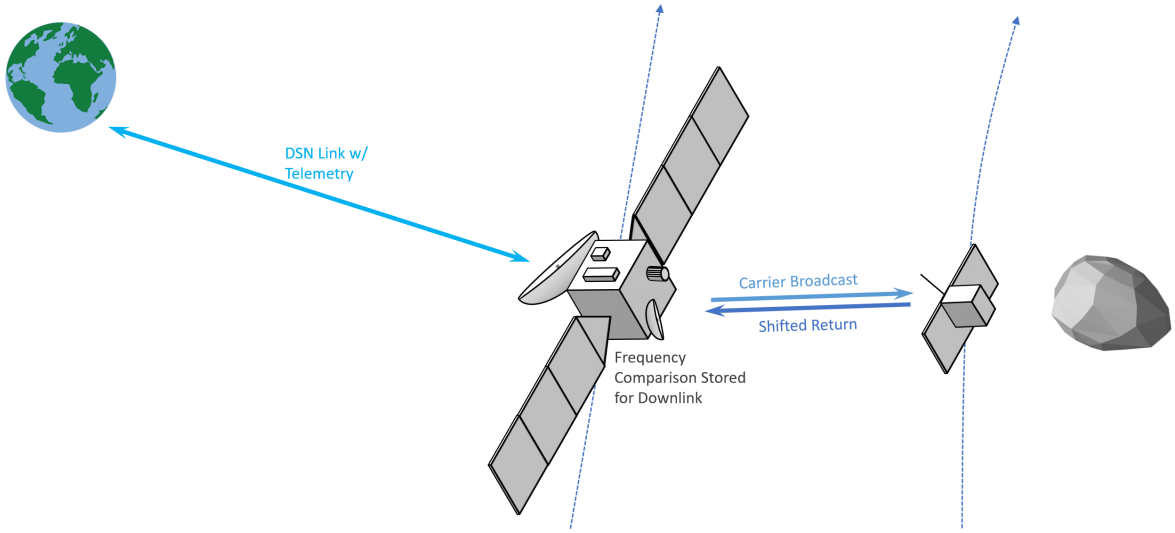

Figure 1: Overview of the DopGrav concept. One or more CubeSats are deployed weeks before the encounter with the asteroid and are tracked optically and radiometrically by the host spacecraft, significantly improving the sensitivity of a mass measurement.

"The factor of three difference in asteroid response between the non-porous and porous cases illustrates the importance of quantifying a body's material properties prior to deploying an impulsive deflection method." [14]

Collectively, this research indicates that it would be very difficult to confidently design an effective kinetic or nuclear mitigation without first knowing the asteroid's mass and porosity.

Methods of Measuring Asteroid Mass: There are many demonstrated methods for measuring asteroid mass; however, most of them are not sensitive, accurate, or rapid enough for PHAs. We note those approaches here: using meteorite analogs [15], observing the gravitational interaction between neighboring asteroids [16], observing binary systems [17], and fusing radar and thermal data to estimate the Yarkovsky acceleration [18].

The only current practical method for determining a small (i.e., 140m) PHA's mass is to send a spacecraft to orbit it. By tracking the spacecraft throughout its orbit around the asteroid, rendezvous encounters provide high-order gravity fields. The challenge is that any specific asteroid target may only offer a rare launch opportunity once every several years and require substantial spacecraft propellant.

Like rendezvous encounters, a spacecraft can be tracked as it flies past an asteroid. Here, instead of using many days or weeks of orbit data to determine the mass, the data arc is limited to a single encounter. The primary observable signal is

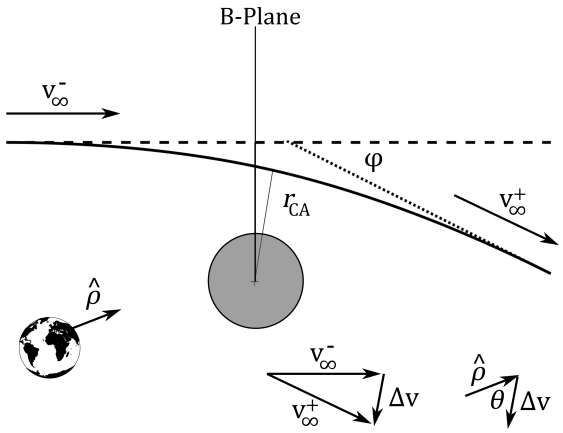

Figure 2: Hyperbolic flyby geometry.

a change in the spacecraft's heliocentric velocity, Δv. Figure 2 depicts the hyperbolic geometry of a spacecraft flying by an asteroid. The magnitude of the Δv is a function of the flyby velocity v_∞, the universal gravitational constant G times the asteroid mass M, and the flyby close approach distance r_{CA}:

$$\Delta v = \frac{2GMv_\infty}{r_{CA}\, v_\infty^2 + GM} \approx \frac{2GM}{r_{CA}\, v_\infty} \qquad (1)$$

(Here, we simplify the expression by noting that $r_{CA}\, v_\infty^2 \gg GM$.)

To give scale to this equation, Figure 3 plots contours of Δv in mm/s over asteroid size and flyby

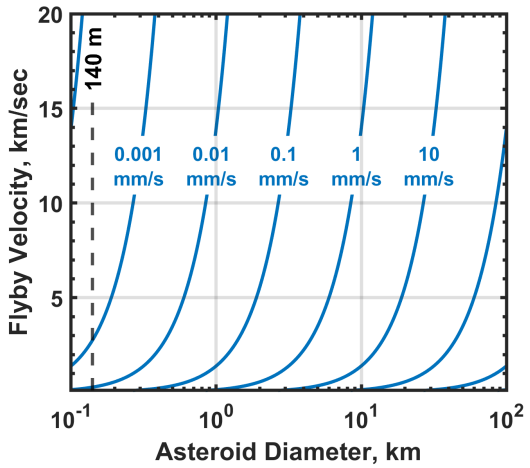

Figure 3: Contours of Total Flyby Δv. Each contour models the Δv for an altitude of 1 body radii above a 2 gm/cm^3 dense asteroid.

speed. This figure depicts the best-case magnitude of Δv that could be expected because the close approach distance is taken to be only 1 body radius above the surface. This is very close to the body's surface, in contrast to most previous flyby missions. The log-scale highlights that small asteroids require orders-of-magnitude more sensitive measurements compared to larger asteroids. Even under these best-case circumstances, a 140 m asteroid requires an effective sensitivity on the order of 0.0001 to 0.001 mm/s.

The spacecraft is tracked before and after the encounter by ground stations, such as the Deep Space Network (DSN). The most informative measurement is the Doppler signal, which is effectively a direct measure of the Δv along the line-of-sight from the station to the spacecraft. One challenge is that a component of the Δv may be unobservable if it is perpendicular to this direction, further reducing the observed signal. Defining θ as the angle between the Δv and the range direction, the observable Δv is

$$\Delta \mathrm{v}_{obs} = \Delta \mathrm{v} \, \cos\theta \tag{2}$$

Rearranging the above equation, the mass measurement is then:

$$M = \frac{\Delta \mathrm{v} \, \cos\theta \, r_{CA} \, v_\infty}{2G} \tag{3}$$

The only term in this mass measurement equation that is easily tailorable is the close-approach distance. The flyby speed and geometry (θ) are predominantly dictated by the orbit mechanics of the encounter. However, decreasing the close-approach distance diminishes other important flyby observations, such as imaging science. The closer the spacecraft goes to the asteroid, the higher the required slew rates and accelerations. Imaging science requires a close approach range within the spacecraft's attitude capability, which is typically 10's or 100's of km.

DopGrav: Based on previous research, the most promising approach for solving this challenge is to employ relative measurements. Relative measurements are generated between two sensing platforms tracking each other or a common target. They offer at least three important advantages:

- *Tailored Geometry*: The inter-spacecraft measurement geometry can be tailored relatively easily because the separation distance is so short. This removes measurement losses due to the encounter geometry (*e.g.*, non-zero θ).
- *Common Errors*: Common errors cancel out in the relative measurements, mitigating the effect of some sources of uncertainty (*e.g.*, asteroid center-of-mass error).
- *Increased Precision*: For some measurement types, the shorter baseline improves measurement precision. For example, a PHA might perturb a spacecraft by only 50 m in a representative flyby scenario. If we attempted to remotely measure that change from a range of approximately 1 AU, the position change would not be observable from even Hubble's highest resolution instrument by an order of magnitude. However, if observed from only 100 km away, it is easily resolvable using existing telescopes like DART's DRACO instrument.

These features of relative measurements are well understood and demonstrated. The Gravity Recovery and Climate Experiment (GRACE) and Gravity Recovery and Interior Laboratory (GRAIL) missions used radiometric measurements between pairs of spacecraft to produce high degree gravity fields of the Earth [19] and Moon [20], respectively.

In asteroid rendezvous encounters, relative optical measurements have proven valuable. The Hayabusa2 mission deployed and tracked target markers (and a rover) in orbit around Ryugu to better determine the gravity field and to estimate local density variations [21, 22]. Likewise, the OSIRIS-REx mission opportunistically imaged and

tracked particles ejected by Bennu. These measurements were used to significantly improve the gravity model [23, 24, 25].

None of these techniques have been operationally applied to high-speed flyby encounters yet. In this study, we assess the performance of relative Doppler measurements in the reconnaissance flyby of 2023 PDC. (We call this approach "DopGrav"). Our prior work has shown that using relative optical measurements ("OpGrav") of passive test-masses can measure the mass of asteroids as small as 400-500 m in diameter (see, *e.g.* [26]). For the purposes of this PDC exercise, that leaves little-to-no margin if 2023 PDC turns out to be on the small end of the size uncertainty. Christensen et al. [27] showed that relative measurements with GRAIL-like inter-satellite Doppler measurement precision can measure the mass of asteroids as small as 100 m in diameter. We assert that achieving such measurement precision would likely require two highly sophisticated spacecraft. Alternatively, this study includes a CubeSat-based test-mass, which would be a relatively simple add-on to a flyby reconnaissance mission. The CubeSats are able to conduct small maneuvers to achieve a low altitude flyby as post-deployment orbit determination updates are made available.

2023 PDC Exercise Scenario: This analysis uses the 2023 Planetary Defense Conference exercise as the context for assessing the proposed system's mass determination performance. The exercise is carefully designed to be a realistic representation of a potential encounter, incorporating accurate physics and response options. The full scenario is documented online[1], but we summarize the key events here. An asteroid is detected in January 2023 with a projected Earth impact risk in 2036. The asteroid is designated '2023 PDC' and has a measured intrinsic magnitude of H = 19.4 $\pm$ 0.3, which corresponds to a most likely size range of 220 to 660 meters in diameter. The asteroid's orbit is summarized in Table 1 and plotted in Figure 4.

The PDC exercise presents an option for a reconnaissance flyby mission that can be launched in October 2024 with a flyby encounter on 1 December 2025. For a Falcon Heavy, the expected launch capability is roughly 500 kg, compatible with the system we evaluate here. The encounter has a relative velocity of 1.7 km/s with an approach solar phase angle (Sun-asteroid-spacecraft angle) of 110 deg. As seen in Figure 4, the mission launches

[1] https://cneos.jpl.nasa.gov/pd/cs/pdc23/

Table 1: 2023 PDC Orbit

Element	Value
Period	359.2 day
Perihelion	0.903 AU
Aphelion	1.075 AU
Inclination	15.37 deg
Right Ascension of Ascending Node	340.86 deg
Argument of Perihelion	308.97 deg

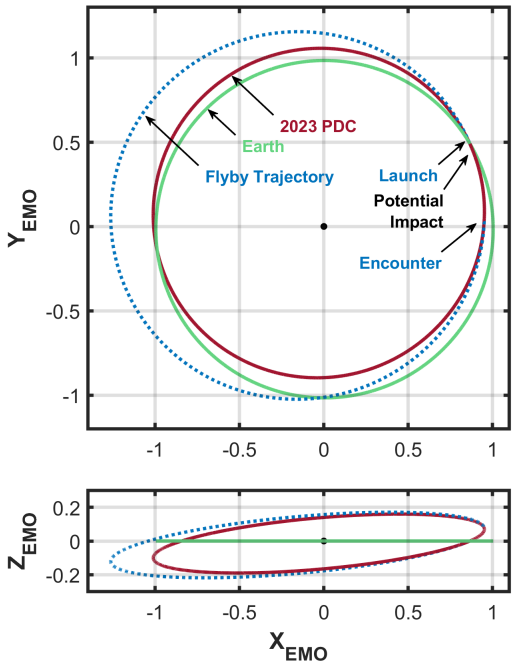

Figure 4: 2023 PDC and reconnaissance mission orbits in the heliocentric ecliptic frame.

at the node-crossing of the asteroid, which is also where the potential impact occurs. Despite the short development time (launch is only 18 months after discovery), the Earth impact is already certain at the time of launch. The primary purposes of the reconnaissance mission is to refine the impact location, characterize the expected impact effects, and support the design of a mitigation mission. To this end, mass is an important parameter to characterize. Prior to the reconnaissance flyby, the range of potential mass values spans three orders of magnitude. In fact, the highest possible mass value is 3000 times the smallest possible value.

Spacecraft Design: In the PDC scenario, the reconnaissance spacecraft is meant to launch only 18 months after first detecting the asteroid. This suggests that the spacecraft will need to be rela-

Table 2: Spacecraft Visible Imager Parameters

Parameter	Value
Aperture	20.8 cm
F#	12.6
Field-of-View (FOV)	0.29 deg (full angle)
Pixel (FOV)	4.96 urad (binned)

tively simple and will likely have been designed and built prior to the detection of the 2023 PDC threat.

For this study, we envision a 120 kg spacecraft bus that includes two instruments: a narrow field-of-view telescope comparable to the DRACO imager flown on DART [28], and a single 12 kg 6U CubeSat with a transponder for the gravity science experiment. Here, the mass of the CubeSat is kept separately from the host spacecraft, so the total system mass is 132 kg. The CubeSat is inspired by the success of the LICIACube mission, which accompanied DART, flying past the Didymos system and returning important post-impact data [3].

Both the host spacecraft and the CubeSat have reaction wheels for attitude control. (We don't model any desaturation maneuvers in this scenario, but include a small value for process noise.) They also both have a chemical propulsion system for small maneuvers. In the case of the CubeSat it is likely a cold gas system since the Δv requirements are low (less than 10 m/s). The spacecraft has two antennas–one for Earth tracking and one for the CubeSat link. Both links use X-Band, though the results are not especially sensitive to this choice.

For the purposes of this study, we model the visible imager with values given in Table 2.

Inter-Satellite Link: The key enabling technology for DopGrav is an inter-satellite RF link between the CubeSat test-mass(es) and the host spacecraft that provides Doppler and ranging measurements. Such technology is not new; missions such as the Gravity Recovery and Climate Experiment (GRACE) and Gravity Recovery and Interior Laboratory (GRAIL) used extremely high precision inter-satellite ranging instruments to measure the range between two spacecraft to determine the gravitational field of the Earth and Moon, respectively [19, 20]. Such instruments require two dedicated, fully capable spacecraft, which limits the scenarios in which it is practical to utilize these instruments. There would also be additional challenges to maintain the pointing and clock synchronization requirements for this type of instrument in a deep space asteroid flyby environment. These challenges are likely surmountable, but would require costly development and time.

In contrast, the implementation of DopGrav that we use here is designed to be relatively inexpensive and straightforward to add to an existing flyby reconnaissance mission. They trade the ultra-high precision of a GRACE or GRAIL-like instrument for speed, cost, and flexibility. The DopGrav instrument as already designed could be constructed and flown in the near future.

In the simplest implementation, the link does not transmit any spacecraft data, and instead only consists of a signal to enable Doppler and ranging measurements. Doppler and range can be estimated by using standard radiometric navigation techniques. The test-mass would include a S-band telemetry, tracking and command (TT&C) transponder that is capable of carrier coherency and ranging. The host spacecraft will transmit a residual carrier deep space ranging waveform. The radio on the test-mass will receive and track the host spacecraft's carrier f_T. It will then turn around the received carrier offset f_R to its transmit channel. The host spacecraft receives and tracks the transmission from the test-mass. It estimates 2-way Doppler by measuring the difference between the nominal test-mass transmit frequency and the received frequency. The received frequency is a function of the relative range rate $\dot{\rho}$, the speed of light c, the transmit frequency f_T, and the transponder ratio ratio γ:

$$f_R = \gamma f_T \left(1 - 2\frac{\dot{\rho}}{c}\right) \tag{4}$$

Similar to coherency, the test-mass transponder will receive the ranging waveform being transmitted by the host spacecraft, lock on to it, and then modulate the recovered ranging waveform onto its transmitted carrier. The host spacecraft receives this turned around ranging signal and compares it to the ranging waveform it originally sent. The measured time difference between the transmitted and received ranging waveforms estimates the 2-way light time between the host spacecraft and test-mass.

Simulations of relevant hardware and link conditions showed a measured coherency precision of approximately 10^{-13} parts for a 60 second integration, indicating an expected velocity error $<$0.1 mm/s. The precision of ranging is expected to be better than 50 ns corresponding to a range error of $<$10 m.

Table 3: Encounter Tracking Schedule

Modality	Schedule
DSN	1 meas per minute continuously to available ground station
OpNav	12 meas 3x per day 120 meas 3x per day in closest 2 days
OpGrav	3 meas every hour 30 meas every hour in closest 2 days
DopGrav	1 meas per minute continuously

Encounter Concept-of-Operations: Our simulation begins 30 days prior to the close approach. The spacecraft's narrow field-of-view telescope could likely detect the asteroid prior to this point, but given the uncertainties in the asteroid's properties, we conservatively assume usable optical navigation images aren't available until 14 days prior to encounter. At the start of the simulation, the spacecraft is targeted to fly past the asteroid 1000 km on the Sunward side. This large distance is meant to represent the accumulation of trajectory errors and asteroid orbit uncertainty up to this point in the encounter. After two days of optical navigation images, the 12 kg CubeSat is deployed 12 days prior to the encounter, using a 10 cm/sec separation spring. (This also causes a small reaction force on the 120 kg host spacecraft.) Once separated, the host begins continuous radiometric tracking to the CubeSat. Both the host and the CubeSat execute a final targeting maneuver 5 days prior to the encounter. The host targets a 50 km miss distance and the CubeSat targets a miss distance of 1 body radius.

Figures 5 and 6 show the encounter geometry. The host targets a final close approach of 50 km on the Sunward side. This is meant to achieve high resolution images while also capturing the sunlit outline of the body for shape reconstruction. The CubeSat targets the same plane and time of close-approach so that the asteroid's perturbation is maximally observable. That is, the host, CubeSat, and asteroid ideally all lie in a line at the time of close-approach. In terms of the gravity experiment, the CubeSat could pass on either side of the asteroid, but we selected the nearer side to reduce any real or perceived risk of impact.

The tracking schedule is summarized in Table 3.

Simulation Setup: We used Ansys Government Initiative's (AGI's) Orbit Determination Toolkit (ODTK) for generating and processing the simulated measurements to quantify the system's expected performance. The scenario covers approximately five weeks around the flyby reconnaissance mission's close approach with 2023 PDC, from 1 November 2025 to 8 December 2025. Table 4 gives the key dates for the encounter scenario. Our force model consists of gravity from the Sun, Earth, Moon, and 2023 PDC, solar radiation pressure, and the planned impulsive maneuvers by both the host spacecraft and the test-mass. SRP is modeled using the spherical cannonball approximation. During the encounter, both spacecraft will have nearly fixed attitudes relative to the Sun, making this a reasonable approximation. Table 5 summarizes the key physical parameters of both spacecraft. In generating the truth trajectories, we assumed a 500 m equivalent mean diameter asteroid with a density of 2 g/cm^3, which is roughly in the middle of the most likely range on the first day of the exercise. The Host spacecraft targets a flyby at a radius of 50 km, distant enough to allow for imaging science. The Test-mass targets a flyby radius of 500 m, which is one body radii above the surface of the 500 m diameter asteroid. For the purposes of our study, we assume both spacecraft achieve their desired flyby states.

Table 4: Key Simulation Dates

Event	Date (UTC)
First OpNav Images	15 Nov 2025 00:00:00
Test-mass Deployment	19 Nov 2025 00:14:25
Maneuvers	26 Nov 2025 00:02:25
Close Approach	01 Dec 2025 00:02:25.900

Table 5: Spacecraft and Test-mass Parameters

Parameter	Value
Host Spacecraft Mass	120 kg
Host Spacecraft Area	5 m^2
Host Spacecraft C_R	1
Test-mass Mass	12 kg
Test-mass Area	1 m^2
Test-mass C_R	1
Host Spacecraft Flyby Radius	50 km
Test-mass Flyby Radius	0.5 km

In addition to the inter-satellite Doppler and ranging measurements provided by the RF link, we also include ground-based DSN tracking of the host spacecraft, optical navigation measurements from the host spacecraft to 2023 PDC, and optical measurements of the test-mass from the host spacecraft (OpGrav). For both types of optical measurements, we assume that additional ground-based processing has been performed on imaged downlinked from the host spacecraft to compute centroids of the respective image targets and provide

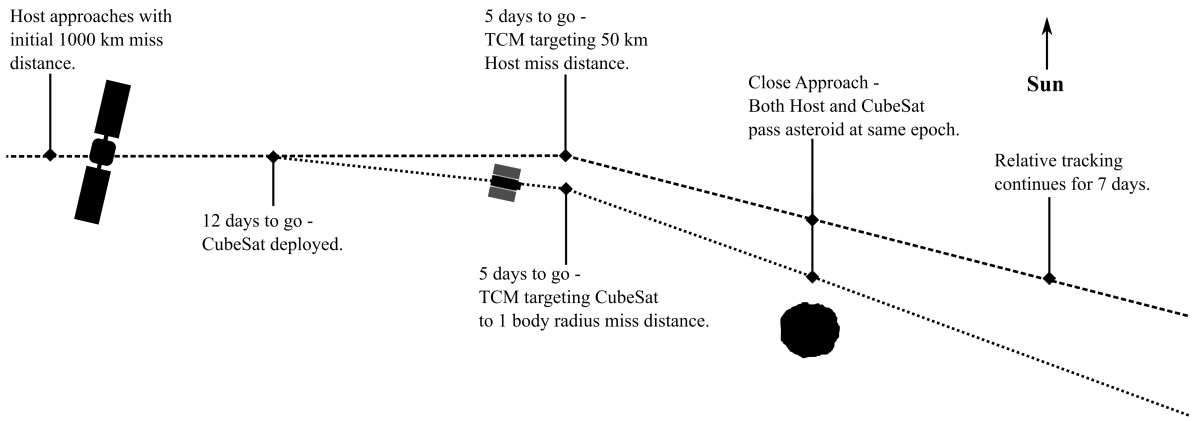

Figure 5: Encounter geometry and maneuver timeline (not to scale).

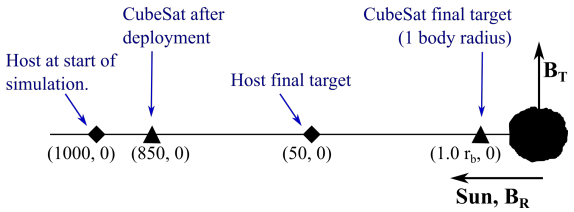

Figure 6: Approach B-Plane targets (not to scale).

Table 6: Measurement Noise Parameters

Parameter	1σ Value
DSN TCP Bias	0.2
DSN TCP White Noise	0.003
DSN Sequential Range Bias	1.5 m
DSN Sequential Range White Noise	0.5 m
Optical White Noise	0.206 arcsec
Inter-satellite Ranging	10 m
Inter-satellite Doppler	0.01 cm/s

right ascension and declination measurements to the filter (see [29] for examples of how this might be done). Table 6 gives the noise parameters modeled for each measurement type.

The filter solves for the position, velocity, and SRP coefficient for both the host and test-mass, the ΔV for the impulsive targeting maneuvers, corrections to the asteroid's orbit, and the asteroid's GM value, where G is Newton's gravitational constant and M is the mass of the asteroid. To initialize the covariance of the host spacecraft, we first simulated a standard DSN-based tracking and orbit determination process for the deep-space cruise portion of the trajectory up to 1 November 2025. The final covariance matrix at the end of this arc is used to initialize our encounter simulation.

Table 7: Estimation Filter Parameters

Parameter	Value
True Asteroid GM	8.73 km^3/s^2
Initial Uncertainty of GM	50% 1σ
Test-mass Deployment ΔV Uncertainty	1 cm/s 1σ
Maneuver Pointing Uncertainty	0.5 deg 1σ
Maneuver Magnitude Uncertainty	0.5% 1σ
Host Spacecraft Initial C_R Uncertainty	5%
Test-mass Initial C_R Uncertainty	20%

The covariance for 2023 PDC at the 1 November 2025 epoch was provided by the PDC organizers.

Results: We present here a summary of the results from our simulation using the configuration previously described. Figure 7 shows the measurement residual ratios (residuals scaled by their 1σ value) for all the measurement types. The majority fall within $\pm 3\sigma$, which is expected for a properly tuned estimation filter. Figure 8 gives the 3σ uncertainties for the Host and Test-mass position and velocity over the course of the encounter. Figure 9 similarly gives the uncertainties in the corrections to the asteroid's ephemeris. Jumps can be seen in the uncertainties for all three objects at the times corresponding to the key events in 4. When the first OpNav images begin, the uncertainties in the asteroid's orbit and the Host spacecraft's state decreases significantly due to the presence of the relative measurements. The asteroid's uncertainties begin coming down before this, because we are using an asteroid-centered frame. In this frame, tracking the Host spacecraft from Earth with the DSN also provides information about the asteroid's orbit. At the time of the Test-mass deployment the uncertainties in the host state jump

Table 8: Sensitivity to Asteroid Size

Asteroid Mean Diameter (m)	True GM (km^3/s^2)	Estimated GM 1σ (%)
300	1.88	2.9
500	8.73	1.6
800	35.78	0.4

up as the deployment acts similarly to a maneuver with uncertainty. There is another large jump when the actual maneuvers take place, as well as a drop at close approach.

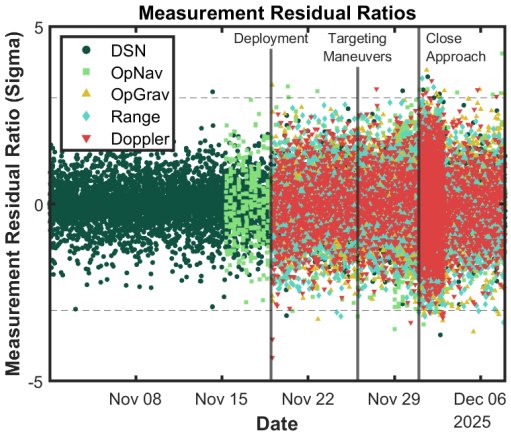

Figure 7: Post-fit measurement residuals for all measurement types. The residuals are scaled by their respective 1σ values to allow for plotting on the same axes.

Lastly, Figure 10 gives the 1σ uncertainty in the asteroid's GM value over the encounter. As expected, the uncertainty in GM does not change at all from its initial value until close approach, at which time it drops significantly as the tracking of the Test-mass provides information about how the Test-masses trajectory was deflected. The initial drop gives a 1σ uncertainty in GM of about 1.6%, which is a substantial improvement.

Analysis:

We repeated our simulation with two additional asteroid sizes; 300 m and 800 m equivalent mean diameter. For each respective asteroid size, the Test-mass's flyby altitude is set to one body radii, i.e. 150 m flyby altitude for the 300 m diameter asteroid and 400 m flyby altitude for the the 800 m diameter asteroid. This matches the altitude choice for the 500 m diameter asteroid used in the previous sections. Table 8 gives the true GM value for each size asteroid and the 1σ uncertainties computed by the filter.

In the exercise scenario, 800 m is the actual diameter of 2023 PDC. We note that this is large enough that optically tracking simple passive test-masses (i.e. OpGrav) could also measure the mass of 2023 PDC to better than 20% 1σ [26]. However, OpGrav would not be able to measure 2023 PDC if it had been on the smaller end of the size range that was predicted at the time the reconnaissance mission was launched. The increased sensitivity of DopGrav, despite the more complex test-mass, makes it better suited for applications to asteroids of this size range.

In either case, 2023 PDC is still much too small to be able to measure its mass using traditional techniques during a flyby, making it necessary to augment the reconnaissance spacecraft with something like DopGrav. The CubeSat-based implementation of DopGrav used here likely would not be able to measure the mass of the smallest high priority PHAs below 140 m in diameter except with very favorable flyby conditions. However, the work by Christensen et al. [27] shows that with increased inter-satellite Doppler precision, it should be possible to measure the mass of these smaller targets. There is therefore a menu of options available for reconnaissance missions to PHAs. Larger asteroids in the size range of the 2023 PDC exercise can be surveyed by the less complex DopGrav implementation presented here, or potentially with the even simpler OpGrav. Smaller asteroids can be surveyed with more complex spacecraft to enable the measurement precision necessary.

Conclusion: The 2023 PDC scenario is meant to be a realistic, accurate threat exercise. The coordinators include an option for a reconnaissance flyby mission arriving in late 2025, however the most likely size range for the 2023 PDC asteroid is such that this reconnaissance mission would not be able to measure the mass of the asteroid by conventional means. The mass, combined with density and porosity, is a key parameter in predicting both the the damage from an impact and for planning the mitigation strategy. We analyzed augmenting the flyby spacecraft with a CubeSat with a transponder, providing inter-satellite Doppler and ranging measurements that enable a mass measurement. The CubeSat is deployed weeks prior to the encounter and tracked by the host spacecraft using the relative Doppler and ranging measurements, as well as relative optical measurements. The CubeSat targets a very low close-approach altitude of only 1 body radii. The short flyby range produces a measurable Δv due to the gravity of the asteroid. At the first epoch of the PDC sce-

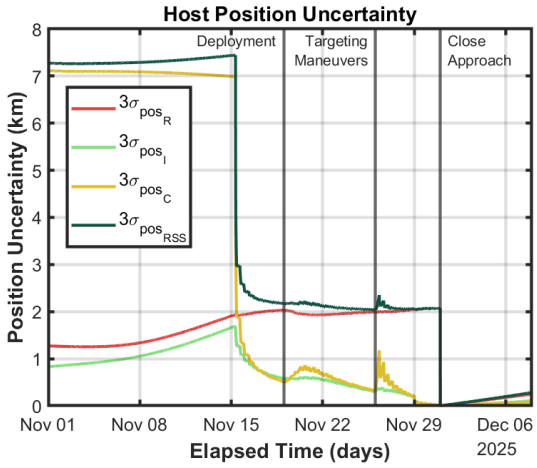

(a) Host Position Uncertainty

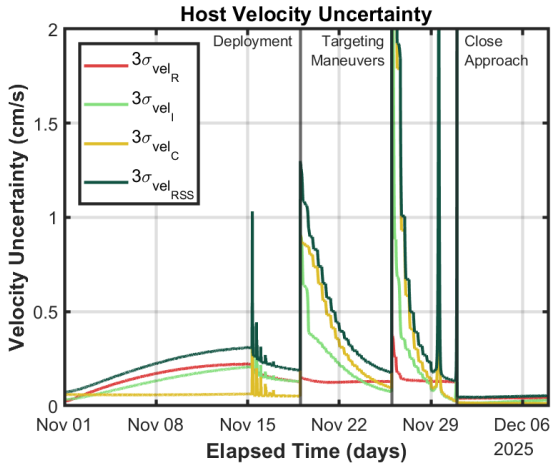

(b) Host Velocity Uncertainty

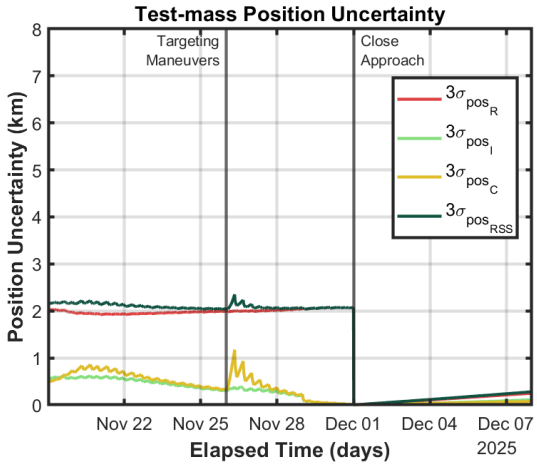

(c) Test-mass Position Uncertainty

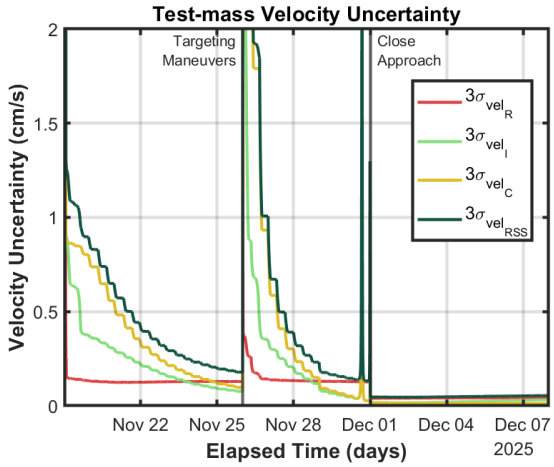

(d) Test-mass Velocity Uncertainty

Figure 8: 3σ position and velocity uncertainties for the host spacecraft and test-mass during the encounter.

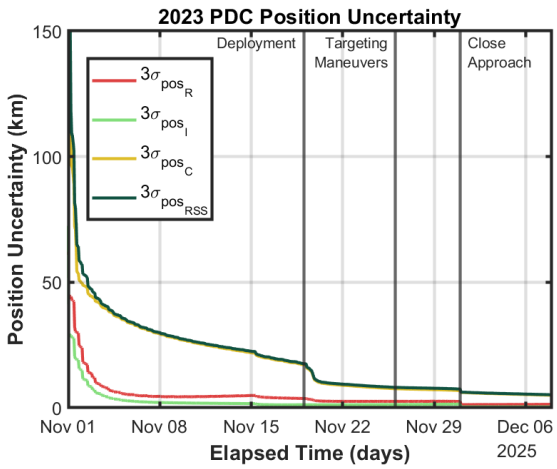

(a) 2023 PDC Position Uncertainty

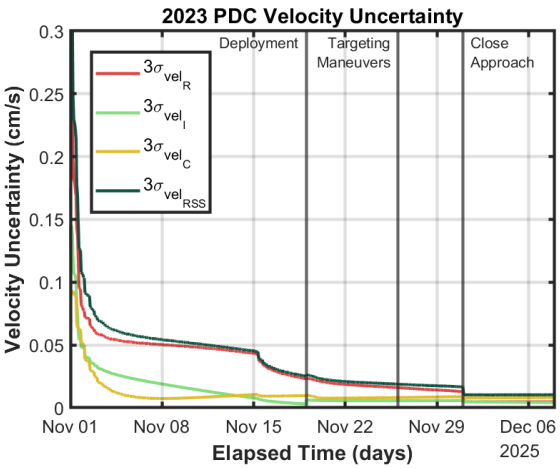

(b) 2023 PDC Velocity Uncertainty

Figure 9: 3σ position and velocity uncertainties for 2023 PDC during the encounter.

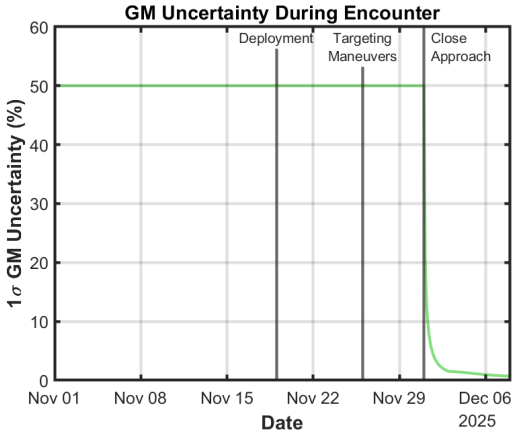

Figure 10: 1σ **uncertainty in the asteroid's** GM **quantity over the encounter.**

nario, the most likely size of the asteroid is 500 m in diameter. Our simulations indicate that the mass of this asteroid could be measured to 1.6% 1σ. The actual asteroid turns out to be 800 m in diameter, which could have the mass measured to 0.4% 1σ. Coupled with a shape model, this would provide a usable density and porosity estimate, which would prove important for predicting the impact effects and designing a mitigation.

These results are extremely encouraging, and they show that a relatively simple implementation of DopGrav would greatly enhance the functionality of reconnaissance flyby missions. However, there are effects we did not include in this work that would need to be studied to fully understand the capabilities and limits of this version of DopGrav. We did not address how the precise targeting of the test-mass's close approach is performed. This would be a significant operational challenge in practice, which may necessitate some level of autonomy on-board the test-mass. We additionally assumed that both spacecraft are not very noisy (e.g. minimal momentum dumps or attitude slews) and that we had a very generous tracking schedule. We also did not study the effects of the asteroid's spin state or attempt to observe higher order gravitational terms. All of these effects pose challenges, and could interfere with the quality of the mass measurement.

The scenario itself is well-suited to this type of DopGrav: 2023 PDC is relatively large for a newly discovered PHA and the flyby speed is slow, both significant factors in making a mass measurement possible. Neither of these are guaranteed in a real threatening asteroid scenario, and more work would need to be done to better quantify the sensitivities of DopGrav to these parameters. Despite this and the aforementioned remaining challenges, we have shown that DopGrav would be a useful tool in the PD toolbox for quickly characterizing a PHA and returning critical measurements that otherwise would not be possible.

Acknowledgments:
We would like to acknowledge the assistance of Brent Barbee and Paul Chodas in providing inputs for the PDC scenario.

References: [1] National Academies of Sciences, Engineering, and Medicine (2022) *Origins, Worlds, and Life: A Decadal Strategy for Planetary Science and Astrobiology 2023-2032* The National Academies Press, Washington, DC ISBN 978-0-309-47578-5 doi. [2] B. Barbee (2020) in *Small Body Assessment Group* Pasadena, CA. [3] E. Dotto, et al. (2021) *Planetary and Space Science* 199:105185 ISSN 0032-0633 doi. [4] P. Miller, et al. (2015) in *IAA Planetary Defense Conference* ARC-E-DAA-TN21736. [5] L. Foschini (1998) *Astronomy and Astrophysics* 337. [6] P. Brown, et al. (2016) *Icarus* 266:96. [7] D. L. Mathias, et al. (2017) *Icarus* 289:106. [8] Y. B. Zel'Dovich, et al. (2002) *Physics of shock waves and high-temperature hydrodynamic phenomena* Courier Corporation. [9] M. B. Syal, et al. (2016) *Icarus* 269:50. [10] K. A. Holsapple, et al. (2012) *Icarus* 221(2):875. [11] M. Jutzi, et al. (2010) *Icarus* 207(1):54. [12] G. J. Flynn, et al. (2015) *Planetary and Space Science* 107:64. [13] D. Gennery (2004) in *2004 Planetary Defense Conference: Protecting Earth from Asteroids* 1439. [14] M. B. Syal, et al. (2013) *Acta Astronautica* 90(1):103. [15] D. T. Britt, et al. (2003) *Meteoritics & Planetary Science* 38(8):1161. [16] J. L. Hilton (2002) *Asteroids III* 1:103. [17] B. Carry (2012) *Planetary and Space Science* 73(1):98. [18] D. Vokrouhlicky, et al. (2015) *Asteroids IV* 509–531. [19] B. D. Tapley, et al. (2004) *Science* 305(5683):503. [20] A. S. Konopliv, et al. (2014) *Geophysical Research Letters* 41(5):1452. [21] H. Takeuchi, et al. (2020) *Astrodynamics* 4:377. [22] S. Kikuchi, et al. (2021) *Icarus* 358:114220. [23] E. Mazarico, et al. (2019) in *AGU Fall Meeting* GSFC-E-DAA-TN76433. [24] S. Chesley, et al. (2020) *Journal of Geophysical Research: Planets* 125(9). [25] D. Scheeres, et al. (2019) in *European Planetary Science Congress/Division for Planetary Sciences Joint Meeting (EPSC-DPS 2019)*. [26] R. Bull, et al. (2021) *Planetary and Space Science* 205 doi. [27] L. Christensen, et al. (2021) *Journal of Spacecraft and Rockets*. [28] Z. J. Fletcher, et al. (2018) in *Space Telescopes and Instrumentation 2018: Optical, Infrared, and Millimeter Wave* vol. 10698 602–612 SPIE. [29] W. M. Owen Jr (2011) in *AAS/AIAA Astrodynamics Specialist Conference*.